

3He and Universe parallelism.

G.E. Volovik

*Low Temperature Laboratory, Helsinki University of Technology, Box 2200, FIN-02015 HUT, Espoo, Finland
and*

Landau Institute for Theoretical Physics, Moscow, Russia

(June 4, 2018)

We discuss topological properties of the ground state of spatially homogeneous ensemble of fermions. There are several classes of topologically different fermionic vacua; in each case the momentum space topology of the vacuum determines the low-energy (infrared) properties of the fermionic energy spectrum. Among them there is class of the gapless systems which is characterized by the Fermi-hypersurface, which is the topologically stable singularity. This class contains the conventional Landau Fermi-liquid and also the non-Landau Luttinger Fermi-liquid. Another important class of gapless systems is characterized by the topologically stable point nodes (Fermi points). Superfluid $^3\text{He-A}$ and electroweak vacuum belong to this universality class. The fermionic quasiparticles (particles) in this class are chiral: close to the Fermi points they are left-handed or right-handed massless relativistic particles. Since the spectrum becomes relativistic at low energy, the symmetry of the system is enhanced in the low-energy edge. The low-energy dynamics acquires local invariance, Lorentz invariance and general covariance, which become better and better when the energy decreases. Interaction of the fermions near the Fermi point leads to collective bosonic modes, which look like effective gauge and gravitational fields. Since the vacuum of superfluid $^3\text{He-A}$ and electroweak vacuum are topologically similar, we can use $^3\text{He-A}$ for simulation of many phenomena in high energy physics, including axial anomaly. $^3\text{He-A}$ textures induce a nontrivial effective metrics of the space, where the free quasiparticles move along geodesics. With $^3\text{He-A}$ one can simulate event horizons, Hawking radiation, rotating vacuum, conical space, etc.

Contents

		D	$^3\text{He-A}$: Gauge invariance but no general covariance.	7	
I	Introduction	2	E Zero charge effect and Maxwell equations.	8	
II	Manifolds of zeroes.	2	F Why $^3\text{He-A}$ is not perfect.	8	
A	Fermi surface as topological object	2	G Chiral anomaly.	8	
1	Topological stability of Fermi surface	2	H Degeneracy of Fermi point as the origin of the non-Abelian gauge field.	9	
2	Landau Fermi liquid	3	IV	Black hole in $^3\text{He-A}$ film.	9
3	Non-Landau Fermi liquids.	4	A	Gravity by motion of superfluids. Sonic black hole.	9
4	Superconducting transition: from pole to zero	4	B	Simulation of 2D black hole	10
B	Fully gapped systems.	4	C	Vacuum in comoving and rest frames.	11
C	Fermi point	5	D	Hawking radiation	11
1	Systems with Fermi points: $^3\text{He-A}$ and Standard Model	5	E	Discussion.	13
2	Topological invariant for Fermi point	5	V	Rotating vacuum.	13
3	Spin from isospin.	5	A	Unruh effect.	13
D	Fermi line	6	B	Zel'dovich-Starobinsky effect.	13
1	Superconductivity in cuprates.	6	C	Cylindrical geometry.	13
2	Scaling law near zeroes.	6	D	Conical texture with negative angle deficit.	14
3	Topological instability of Fermi line.	6	E	Rotating frame.	14
III	Properties of system with Fermi points.	6	F	Ergoregion in superfluids.	14
A	Relativistic massless chiral fermions.	6	G	Rotating detector.	15
B	Collective modes – electromagnetic and gravitational fields.	7	H	Radiation to the ergoregion.	16
C	Gauge invariance, general covariance, conformal invariance.	7	I	Discussion.	16
		VI	Discussion	16	

arXiv:cond-mat/9902171v3 5 Apr 1999

I. INTRODUCTION

The physical vacuum is a complicated condensed matter [1–4]. At the moment we know only the low-energy properties of this substance, i.e. the properties at energies much smaller than the Planck energy scale, $E \ll E_P = \sqrt{\hbar c^5/G}$, where G is Newton’s constant. We know that at the low-energy edge our vacuum has many different symmetries: $U(1)$ and $SU(3)$ gauge symmetries, Lorentz invariance, general coordinate invariance, and discrete CPT symmetry. With increasing energy more elements of symmetry are added: $SU(2)$ symmetry of weak interactions, probably the GUT symmetry and even supersymmetry. When the temperature decreases such symmetries become spontaneously broken. This is the traditional point of view, which is supported by the observation of the similar symmetry breaking in different (many-body) condensed matter systems: superfluids, superconductors, magnets, liquid and ordinary crystals.

However there is another and actually opposite point of view: all symmetries known in the Universe spontaneously (but without any phase transition) appear at the low-energy corner [5]. They become more and more pronounced the lower the energy. The symmetries disappear at higher energies when the Planck energy is approached. This conjecture is also supported by the condensed matter analogy.

Here we discuss the topological origin of such enhanced symmetry in the infrared limit. It is caused by the so-called topologically stable Fermi points in the spectrum of the fermionic system. We show that if such points exist in quantum condensed matter, then at low enough temperature this system exhibits fully or partially the Lorentz invariance, general covariance, and gauge invariance. Moreover the collective modes which describe such a system at low T all are represented by the chiral relativistic fermions, gauge fields, and gravity. All are the low-energy phenomena, which are absent at higher energies, where the condensed matter has only a very limited set of the global symmetries.

From the second point of view some directions in physics look artificial. In particular, since the gravity exists only as the infrared phenomenon one should not quantize gravity: Only low-energy gravitons can be quantized [6]. The same concerns the multidimensional string theories, which also give rise to gravitation in the infrared limit. The Fermi point mechanism does not require a high dimensionality for the space-time: The topologically stable Fermi point is just a property of the conventional 3+1 dimensional space-time.

II. MANIFOLDS OF ZEROES.

The Fermi point is a particular case of the topologically stable manifolds of zeroes in the fermionic spectrum. Let

us start with the simplest such manifold – the Fermi surface.

A. Fermi surface as topological object

1. Topological stability of Fermi surface

The Fermi surface appears in the noninteracting Fermi gas, where the energy spectrum of fermions is

$$E(p) = \frac{p^2}{2m} - \mu, \quad (1)$$

and $\mu > 0$ is the chemical potential. The Fermi surface bounds the volume in the momentum space where the energy is negative, $E(p) < 0$, and where the particle states are all occupied at $T = 0$. In this isotropic model the Fermi surface is a sphere of radius $p_F = \sqrt{2m\mu}$.

It is important that the Fermi surface survives even if interactions between particles are introduced. Such stability of Fermi surface comes from the topological property of the Feynman quantum mechanical propagator – the one-particle Green’s function

$$\mathcal{G} = (z - \mathcal{H})^{-1}. \quad (2)$$

Let us write the propagator for a given momentum \mathbf{p} and for the imaginary frequency, $z = ip_0$. The imaginary frequency is introduced to avoid the conventional singularity of the propagator ”on the mass shell”, i.e. at $z = E(p)$. For noninteracting particles the propagator has the form

$$G = \frac{1}{ip_0 - E(p)}. \quad (3)$$

Obviously there is still a singularity: On the 2D hypersurface ($p_0 = 0, p = p_F$) in the 4-dimensional space (p_0, \mathbf{p}) the propagator is not well defined. This singularity is stable, i.e. cannot be eliminated by small perturbations. The reason is that the phase Φ of the Green’s function $G = |G|e^{i\Phi}$ changes by 2π around the path embracing this 2D hypersurface in the 4D-space (see Fig. 1). The phase winding number $N = 1$ cannot change continuously, that is why it is robust towards any perturbation. Thus the singularity of the Green’s function on the 2D-surface in the momentum space is preserved, even when interactions between particles are introduced.

Exactly the same topological conservation of the winding number leads to the stability of the quantized vortex in superfluids and superconductors, the only difference being that, in the case of vortices, the phase winding occurs in the real space, instead of the momentum space. The complex order parameter $\Psi = |\Psi|e^{i\Phi}$ changes by $2\pi N$ around the path embracing vortex line in 3D space or vortex sheet in 3+1 space. The connection between

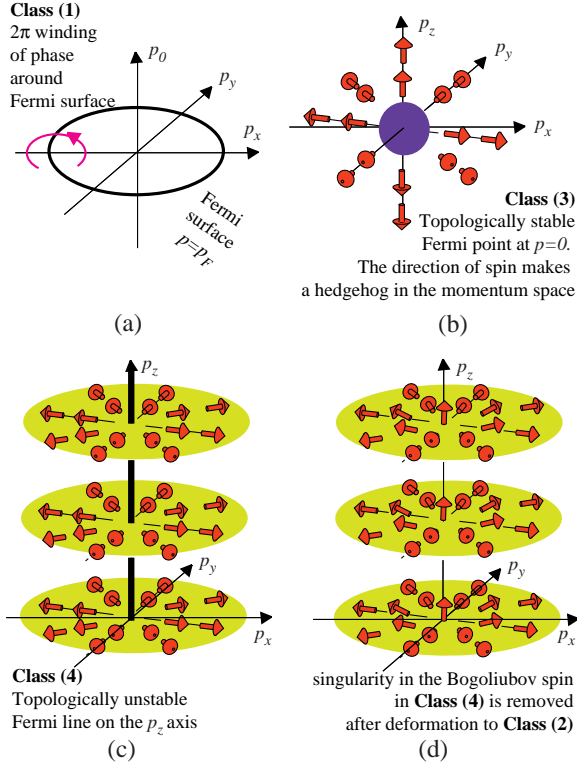


FIG. 1. (a) The Fermi surface in the 2+1 momentum space. For simplicity the p_z coordinate is suppressed so that the Fermi surface is the line $(p_0 = 0, p = p_F)$ in the 2+1 space (p_0, p_x, p_y) . This line is a singularity, which is similar to a vortex in a real 3D-space: The phase of the propagator $G = (ip_0 - (p_x^2 + p_y^2 - p_F^2)/2m)^{-1}$ changes by 2π around the line in the momentum space in the same manner as the phase of the order parameter changes by 2π around a vortex in the real space. In general case the winding number N_1 – the topological invariant of the Fermi surface – is given by Eq.(4). (b) Fermi point at $\mathbf{p} = 0$ in the 3D momentum space (p_x, p_y, p_z) . At this point the particle energy $E = cp$ is zero. A right-handed particle is considered with its spin parallel to the momentum \mathbf{p} , *i.e.* $\mathbf{s}(\mathbf{p}) = (1/2)\mathbf{p}/p$. The spin makes a hedgehog in the momentum space, which is topologically stable. The topological invariant of the Fermi point is $N_3 = 1$, where N_3 is given by Eq.(13). (c) Fermi line – topologically unstable manifold of zeroes – is shown in the 3D momentum space (p_x, p_y, p_z) . The (Bogoliubov) spin (arrows) is confined into the (p_x, p_y) plane and has a singularity on the p_z axis. (d) This singularity can be removed by a continuous transformation. The spin escapes into a third dimension (p_z) and becomes well defined on the p_z axis. As a result, the quasiparticle spectrum becomes fully gapped (the “relativistic” fermion acquires the mass).

the topology in real space and the topology in momentum space is, in fact, even deeper (see *e.g.* Ref. [7]). If the order parameter depends on space-time, the propagator in semiclassical approximation depends both on 4-momentum and on space-time coordinates $G(p_0, \mathbf{p}, t, \mathbf{r})$.

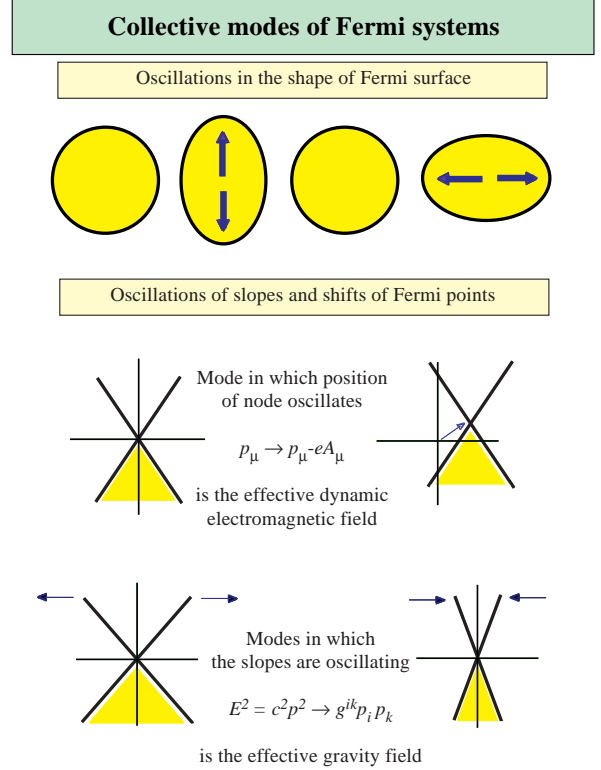


FIG. 2. Collective modes of fermionic systems with Fermi surface and Fermi point.

The topology in the 4+4 dimensional space describes: (i) The momentum space topology in the homogeneous system; (ii) The defects of the order parameter in real space; and (iii) Topology of the energy spectrum within the topological defects [8].

In the more complicated cases, when the Green’s function is the matrix with spin and band indices, the phase of the Green’s function becomes meaningless. In this case one should use a general analytic expression for the integer topological invariant which is responsible for the stability of the Fermi surface:

$$N_1 = \text{Tr} \oint_C \frac{dl}{2\pi i} \mathcal{G}(p_0, p) \partial_l \mathcal{G}^{-1}(p_0, p). \quad (4)$$

Here the integral is taken over an arbitrary contour C in the momentum space (\mathbf{p}, p_0) , which encloses the Fermi hypersurface; and Tr is the trace over the spin and band indices.

2. Landau Fermi liquid

The topological class of systems with Fermi surface is rather broad. In particular it contains the conventional Landau Fermi-liquid, in which the propagator preserves the pole. Close to the pole the propagator is

$$G = \frac{Z}{ip_0 - v_F(p - p_F)}. \quad (5)$$

Evidently the residue $Z \neq 1$ does not change the topological invariant for the propagator, Eq.(4), which remains $N_1 = 1$. This is essential for the Landau theory of an interacting Fermi liquid; it confirms the assumption that in Fermi liquids the spectrum of quasiparticles at low energy is similar to that of particles in a Fermi gas. It is also important for the consideration of the bosonic collective modes of the Landau Fermi-liquid. The interaction between the fermions cannot change the topology of the fermionic spectrum, but it produces the effective field acting on a given particle by the other moving particles. This effective field cannot destroy the Fermi surface owing to its topological stability, but it can locally shift the position of the Fermi surface. Therefore a collective motion of the particles is seen by an individual quasiparticle as a dynamical mode of the Fermi surface. These bosonic oscillative modes are known as the different harmonics of the zero sound. An example is shown in the upper part of Fig.2.

Note that the Fermi hypersurface exists for any spatial dimension. In the 2+1 dimension the Fermi hypersurface is a line – the vortex line in the 2+1 momentum space as is shown in Fig. 1(a).

3. Non-Landau Fermi liquids.

In the 1+1 dimension the Green's function loses its pole, but nevertheless the Fermi surface is still there [9,10]. In 1+1 dimension the Landau Fermi liquid transforms to another states within the same topological class. Example is provided by the Luttinger liquid. Close to the Fermi surface the Green's function for the Luttinger liquid can be approximated as (see [11,9,12])

$$G(z, p) \sim (ip_0 - v_1 \tilde{p})^{\frac{g-1}{2}} (ip_0 + v_1 \tilde{p})^{\frac{g}{2}} (ip_0 - v_2 \tilde{p})^{\frac{g-1}{2}} (ip_0 + v_2 \tilde{p})^{\frac{g}{2}} \quad (6)$$

where v_1 and v_2 correspond to Fermi velocities of spinons and holons and $\tilde{p} = p - p_F$. The above equation is not exact but reproduces the topology of the Green's function in Luttinger Fermi liquid. If $g \neq 0$ and $v_1 \neq v_2$, the singularity in the $(\tilde{p}, z = ip_0)$ momentum space occurs on the Fermi surface, i.e. at $(p_0 = 0, \tilde{p} = 0)$. The topological invariant in Eq.(??) remains the same $N_1 = 1$, as for the conventional Landau Fermi-liquid. The difference from Landau Fermi liquid occurs only at real frequency z : The quasiparticle pole is absent and one has the branch cut singularities instead of the mass shell, so that the quasiparticles are not well defined. The population of the particles has no jump on the Fermi surface, but has a power-law singularity in the derivative [10].

Another example of the non-Landau Fermi liquid is the Fermi liquid with exponential behavior of the residue

[13]. It also has the Fermi surface with the same topological invariant, but the singularity at the Fermi surface is exponentially weak.

4. Superconducting transition: from pole to zero

In this section we do not consider the bifurcations which lead to the overall reconstruction of the particle spectrum, which occur, say, during the transition to superconducting state. We assume that the temperature, though is small compared to the "Planck" scale $E_P = \mu$, is still above the superfluid transition: $T_c < T \ll E_P$. But even in the superconducting region $T < T_c$ the winding number for the conventional Green's function is preserved: the invariant in Eq.(??) is again $N_1 = 1$. Only instead of pole at $p = p_F$ in the Green's function of the normal state, one has zero at $p = p_F$ in the superconducting state:

$$G = -\frac{ip_0 + M(p)}{p_0^2 + M^2(p) + \Delta^2}, \quad M(\mathbf{p}) = \frac{p^2}{2m} - \mu \approx v_F(p - p_F) \quad (7)$$

where Δ is the gap in the quasiparticle spectrum. This demonstrates the stability of the singularity in the Green's function, though the Fermi surface as the manifold of zeroes in the energy spectrum disappears in the superconductor.

B. Fully gapped systems.

Although the systems we have discussed contain fermionic and bosonic quantum fields, this is not the relativistic quantum field theory which we need for the simulation of quantum vacuum: There is no Lorentz invariance and the oscillations of the Fermi surface do not resemble the gauge field even remotely. The situation is somewhat better for superfluids and superconductors with fully gapped spectra; examples, which provide useful analogies with Dirac fermions and spontaneously broken symmetry in quantum fields, are conventional superconductors [14] and superfluid $^3\text{He-B}$ [15]. In $^3\text{He-B}$ the Hamiltonian of free Bogoliubov quasiparticles is the 4×4 matrix:

$$\mathcal{H} = \begin{pmatrix} M(\mathbf{p}) & c\vec{\sigma} \cdot \mathbf{p} \\ c\vec{\tau} \cdot \mathbf{p} & -M(\mathbf{p}) \end{pmatrix} = \tau_3 M(\mathbf{p}) + c\tau_1 \vec{\sigma} \cdot \mathbf{p}, \quad (8)$$

$$c = \frac{\Delta}{p_F}, \quad \mathcal{H}^2 = E^2 = M^2(\mathbf{p}) + \Delta^2, \quad (9)$$

where the Pauli 2×2 matrices $\vec{\sigma}$ describe the conventional spin of fermions and 2×2 matrices $\vec{\tau}$ describe the Bogoliubov isospin in the particle-hole space. The Bogoliubov Hamiltonian asymptotically approaches the Dirac one in

the low p limit. This is however is not the low energy limit, which for the typical ${}^3\text{He-B}$ parameters occurs for p close to p_F . The low p and low E limits coincide at large negative μ , which is not the case in ${}^3\text{He-B}$. Nevertheless the ${}^3\text{He-B}$ also serves as a model system for simulations of many phenomena in particle physics and cosmology including experimental verification [16] of the Kibble mechanism describing formation of cosmic strings in the early Universe [17].

Note that even for the fully gapped systems there can exist the momentum-space topological invariants, which characterize the vacuum states. Typically this occurs in 2+1 systems, e.g. in the 2D electron system exhibiting quantum Hall effect [18]; in thin film of ${}^3\text{He-A}$ (see [19] and Sec.9 of Ref. [20]); and in the 2D superconductors with broken time reversal symmetry [21]. The quantum (Lifshitz) transition between the states with different topological invariants occurs through the intermediate gapless regime [20].

C. Fermi point

1. Systems with Fermi points: ${}^3\text{He-A}$ and Standard Model

Now we proceed to the topological class which most fully exhibits the fundamental properties needed for a realization of the relativistic quantum fields, analogous to those in particle physics and gravity.

It is the class of systems, whose representatives are superfluid ${}^3\text{He-A}$ and the vacuum of relativistic left-handed and right-handed chiral fermions (another example of this class in condensed matter has been discussed for gapless semiconductors [22]). This class is characterized by points in the momentum space where the (quasi)particle energy is zero. In particle physics the energy spectrum $E(\mathbf{p}) = cp$ is characteristic of the massless neutrino (or any other chiral lepton or quark in the Standard Model) with c being the speed of light. The energy of a neutrino is zero at point $\mathbf{p} = 0$ in the 3D momentum space. The Hamiltonian for the neutrino – the massless spin-1/2 particle – is a 2×2 matrix

$$\mathcal{H} = \pm c\vec{\sigma} \cdot \mathbf{p} \quad (10)$$

which is expressed in terms of the Pauli spin matrices $\vec{\sigma}$. The sign $+$ is for a right-handed particle and $-$ for a left-handed one: the spin of the particle is oriented along or opposite to its momentum, respectively.

The Bogoliubov matrix for the ${}^3\text{He-A}$ fermions is

$$\mathcal{H} = \tau_3 M(\mathbf{p}) + c(\vec{\sigma} \cdot \hat{d})(\tau_1 \mathbf{e}^{(1)} \cdot \mathbf{p} - \tau_2 \mathbf{e}^{(2)} \cdot \mathbf{p}), \quad (11)$$

where $\mathbf{e}^{(1)}$ and $\mathbf{e}^{(2)}$ are real vectors, which in equilibrium or ground state are unit orthogonal vectors. The energy of the fermions

$$E_{\mathbf{p}}^2 = M^2(\mathbf{p}) + c^2(\mathbf{p} \times \hat{\mathbf{l}})^2, \quad \hat{\mathbf{l}} \equiv \mathbf{e}^{(3)} = \mathbf{e}^{(1)} \times \mathbf{e}^{(2)}, \quad (12)$$

is zero at 2 points, at $\mathbf{p} = \pm p_F \hat{\mathbf{l}}$.

2. Topological invariant for Fermi point

Let us show that zeroes in the spectrum of the chiral fermions and in the spectrum of ${}^3\text{He-A}$ fermions are topologically stable and described by the same topological invariant. Let us again consider the propagator of the particle $\mathcal{G} = (ip_0 - \mathcal{H})^{-1}$ on the imaginary frequency axis, $z = ip_0$. One can see that this propagator still has a singularity, which is now not on the surface but at the points in the 4D momentum space: $(p_0 = 0, \mathbf{p} = 0)$ and $(p_0 = 0, \pm p_F \hat{\mathbf{l}})$ for chiral fermions and ${}^3\text{He-A}$ fermions respectively. An integer topological invariant which supports the stability of the point zeroes is expressed in terms of the propagator in the following way [20]:

$$N_3 = \frac{1}{24\pi^2} e_{\mu\nu\lambda\gamma} \text{tr} \int_{\sigma} dS^{\gamma} \mathcal{G} \partial_{p_{\mu}} \mathcal{G}^{-1} \mathcal{G} \partial_{p_{\nu}} \mathcal{G}^{-1} \mathcal{G} \partial_{p_{\lambda}} \mathcal{G}^{-1}, \quad (13)$$

where σ is the 3-dimensional surface embracing the point node in the 4-momentum space.

For the chiral fermions in Eq.(10) this invariant is $N_3 = \pm 1$, where the sign is determined by the chirality of the fermion. The meaning of this topological invariant can be easily visualized. Let us consider the behavior of the particle spin $\mathbf{s}(\mathbf{p})$ as a function of its momentum \mathbf{p} in the 3D-space $\mathbf{p} = (p_x, p_y, p_z)$. For right-handed particles $\mathbf{s}(\mathbf{p}) = \mathbf{p}/2p$, while for left-handed ones $\mathbf{s}(\mathbf{p}) = -\mathbf{p}/2p$. In both cases the spin distribution in the momentum space looks like a hedgehog (see Fig. 1b), whose spines are represented by spins: spines point outward for the right-handed particle and inward for the left-handed one. In the 3D-space the hedgehog is topologically stable.

3. Spin from isospin.

For the ${}^3\text{He-A}$ fermions in Eq.(11) $N_3 = \mp 2$, where the sign is determined by the position of the node, $\mathbf{p} = \pm p_F \hat{\mathbf{l}}$. The topological invariant is twice larger because of the double degeneracy of the Fermi point over the conventional spin of the ${}^3\text{He}$ atom. For each projection of spin one has $N_3 = \mp 1$. Note that the Bogoliubov spin $\vec{\tau}$ in ${}^3\text{He-A}$ plays the same role as the conventional spin $\vec{\sigma}$ of chiral fermions in Eq.(10). On the other hand the conventional spin of the ${}^3\text{He}$ atom is responsible for the degeneracy, but not for chirality, and thus plays the part of the isospin (see also Sec.III H). This means that the origin of the spin responsible for the chirality of the (quasi)particle is fully determined by the matrix structure of the Fermi

point. In this sense there is no principle difference between spin and isospin: changing the matrix structure one can convert isospin to spin, while the topological charge of the Fermi point remains invariant.

D. Fermi line

1. Superconductivity in cuprates.

The high-temperature superconductors in cuprates most probably contain zeroes in their quasiparticle energy spectrum. The ARPES experiments [23] show that these are four lines in the 3D momentum space where the quasiparticle energy is zero or, equivalently, four point zeroes in the 2D CuO₂ planes. The high-T superconductors thus belong to class of systems with Fermi lines: the dimension D of the manifold of zeroes is 1, which is intermediate between a Fermi surface with $D = 2$ and a Fermi point with $D = 0$.

The energy spectrum of quasiparticles near each of the 4 gap nodes can be written as

$$\mathcal{H} = \tau_1 c^x (p_x - p_x^{(0)}) + \tau_3 c^y (p_y - p_y^{(0)}) . \quad (14)$$

The "speeds" of light c^x and c^y are the "fundamental" characteristics determined by the microscopic physics of the cuprates. This means that the system belongs to the same class as 2+1 QFT with massless relativistic fermions.

2. Scaling law near zeroes.

As in the other two classes of fermionic systems with the gapless quasiparticles, all low-energy (infrared) properties of cuprate superconductors are determined by zeroes. In particular, the density of the fermionic states is determined by the dimension of the zeroes:

$$N(E) = \sum_{\mathbf{p}} \delta(E - E(\mathbf{p})) \sim E^{2-D} . \quad (15)$$

Many low-temperature properties of these superconductors are obtained from a simple scaling arguments. For example, an external magnetic field B has dimension of E^2 and thus of T^2 . At finite B , the density of states is nonzero even at $E = 0$. Substituting $B \sim E^2$ to Eq.(15) one obtains $N(0, B) \sim B^{(2-D)/2}$ and the following scaling law for the heat capacity:

$$C(T, B) = B^{(2-D)/2} T f\left(\frac{B}{T^2}\right) , \quad (16)$$

where f is some function with the known asymptotes (see [24]). An experimental indication of such scaling with $D = 1$ was reported for YBa₂Cu₃O₇ in Ref. [25].

3. Topological instability of Fermi line.

The lines of zeroes generally have no stability: There is no corresponding N_2 invariant, which can support the topological stability. The singular line in the momentum space from which the spines (now the vector $\vec{\tau}$) point outward (see Fig. 1c) can be eliminated by the escape of the $\vec{\tau}$ -vector to a third dimension. This can be accomplished by an operation similar to the folding of an umbrella (see Fig. 1d).

Existence of the nodal lines can be prescribed, however, by the symmetry of the ground state. There are many nontrivial classes of superconductors, whose symmetry supports the existence of nodal lines in symmetric positions in the momentum space [26]. The symmetry violating perturbations, such as impurities, an external magnetic field, etc., destroy the lines of zeroes [8]. One could expect different types of transformations of these lines of zeroes which depend on the perturbation. Impurities, for example, can : (i) produce the gap in the fermionic spectrum [27] (see Fig.1d), which corresponds to appearance of mass for the 2+1 relativistic fermions; (ii) lead to the finite density of states [28], thus transforming the system to Class (1); (iii) produce zeroes of fractional dimension, which means that the exponent in the density of states $N(E) \propto E^{2-D}$ is non-integral [29] and thus corresponds to a fractional D of the manifold of zeroes; and (iv) lead to localization [30]. An open question is: Can the quantum fluctuations do the same, in particular, can they change the effective dimension of the zeroes?

III. PROPERTIES OF SYSTEM WITH FERMI POINTS.

A. Relativistic massless chiral fermions.

Close to the Fermi point $p_\mu^{(0)}$ in the 4D space one can expand the propagator in terms of the deviations from this Fermi point, $p_\mu - p_\mu^{(0)}$. If the Fermi point is not degenerate, the general form of the propagator is

$$\mathcal{G}^{-1} = \tau^a e_a^\mu (p_\mu - p_\mu^{(0)}) . \quad (17)$$

Here we returned back from the imaginary frequency axis to the real energy, so that $z = E = -p_0$ instead of $z = ip_0$; and $\tau^a = (1, \vec{\tau})$. The quasiparticle spectrum $E(\mathbf{p})$ is given by the poles of the propagator:

$$g^{\mu\nu} (p_\mu - p_\mu^{(0)})(p_\nu - p_\nu^{(0)}) = 0 , \quad g^{\mu\nu} = \eta^{ab} e_a^\mu e_b^\nu . \quad (18)$$

Thus in the vicinity of the Fermi point the massless quasiparticles are described by the Lorentzian metric $g^{\mu\nu}$. It is most important that this is the general form of the energy spectrum in the vicinity of any Fermi point, even

if the underlying Fermi system is not Lorentz invariant; superfluid $^3\text{He-A}$ is an example. The fermionic spectrum necessarily becomes Lorentz invariant near the Fermi point, *i.e.*. If one applies this reasoning to our quantum vacuum, one may conclude that possibly the observed Lorentz invariance of the physical laws is not a fundamental but a low-energy property of the vacuum which results from the existence of the topologically stable Fermi points.

B. Collective modes – electromagnetic and gravitational fields.

Let us consider the collective modes in such a system. The effective fields acting on a given particle due to interactions with other moving particles cannot destroy the Fermi point. That is why, under the inhomogeneous perturbation of the fermionic vacuum the general form of Eqs.(17-18) is preserved. However the perturbations lead to a local shift in the position of the Fermi point $p_\mu^{(0)}$ in momentum space and to a local change of the vierbein e_a^μ (which in particular includes slopes of the energy spectrum (see Fig. 2). This means that the low-frequency collective modes in such Fermi liquids are the propagating collective oscillations of the positions of the Fermi point and of the slopes at the Fermi point. The former is felt by the right- or the left-handed quasiparticles as the dynamical gauge (electromagnetic) field, because the main effect of the electromagnetic field $A_\mu = (A_0, \mathbf{A})$ is just the dynamical change in the position of zero in the energy spectrum: in the simplest case $(E - eA_0)^2 = c^2(\mathbf{p} - e\mathbf{A})^2$.

The collective modes related to a local change of the vierbein e_a^μ correspond to the dynamical gravitational field. The quasiparticles feel the inverse tensor $g_{\mu\nu}$ as the metric of the effective space in which they move along the geodesic curves

$$ds^2 = g_{\mu\nu} dx^\mu dx^\nu \quad (19)$$

Therefore, the collective modes related to the slopes play the part of the gravity field (see Fig. 2).

Thus near the Fermi point the quasiparticle is the chiral massless fermion moving in the effective dynamical electromagnetic and gravitational fields.

C. Gauge invariance, general covariance, conformal invariance.

Another important property which results from the above equation is that the fermionic propagator in Eq.(17) is gauge invariant and even obeys the general covariance near the Fermi point. For example, the local phase transformation of the wave function of the fermion, $\Psi \rightarrow \Psi e^{ie\alpha(\mathbf{r},t)}$ can be compensated by the shift of the

”electromagnetic” field $A_\mu \rightarrow A_\mu + \partial_\mu \alpha$. These attributes of the electromagnetic (A_μ) and gravitational ($g^{\mu\nu}$) fields also arise spontaneously as the low-energy phenomena.

Now let us discuss the dynamics of collective bosonic modes, A_μ and $g^{\mu\nu}$. Since these are the effective fields their motion equations do not necessarily obey gauge invariance and general covariance. However, in some special cases such symmetries can arise in the low energy corner. What are the conditions for that?

The effective Lagrangian for the collective modes is obtained by integrating over the vacuum fluctuations of the fermionic field. This principle was used by Sakharov and Zeldovich to obtain an effective gravity [31] and effective electrodynamics [32], both arising from fluctuations of the fermionic vacuum. If the main contribution to the effective action comes from the vacuum fermions whose momenta \mathbf{p} are concentrated near the Fermi point, *i.e.* where the fermionic spectrum is linear and thus obeys the “Lorentz invariance”, the result of the integration is necessarily invariant under gauge transformation, $A_\mu \rightarrow A_\mu + \partial_\mu \alpha$, and has a covariant form. The obtained effective Lagrangian then gives the Maxwell equations for A_μ and the Einstein equations for $g_{\mu\nu}$, so that the propagating bosonic collective modes do represent the gauge bosons and gravitons.

Thus two requirements must be fulfilled – (i) the fermionic system has a Fermi point and (ii) the main physics is concentrated near this Fermi point. In this case the system acquires at low energy all the properties of the modern quantum field theory: chiral fermions, quantum gauge fields, and gravity. All these ingredients are actually low-energy (infra-red) phenomena.

There is another important symmetry obeyed by massless relativistic Weyl fermions, the conformal invariance – the invariance under transformation $g_{\mu\nu} \rightarrow a(\mathbf{r},t)g_{\mu\nu}$. In the extreme limit when the vacuum fermions are dominantly relativistic, the effective action for gravity must be conformally invariant. Such gravity, the so-called Weyl gravity, is a viable rival to Einstein gravity in modern cosmology [33,34]: The Weyl gravity (i) can explain the galactic rotation curves without dark matter; (ii) it reproduces the Schwarzschild solution at small distances; (iii) it can solve the cosmological constant problem, since the cosmological constant is forbidden if the conformal invariance is strongly obeyed; etc. (see [35]).

D. $^3\text{He-A}$: Gauge invariance but no general covariance.

Let us consider what happens in a practical realization of systems with Fermi points in condensed matter – in $^3\text{He-A}$. Close to the gap nodes, *i.e.* at energies $E \ll \Delta$, where Δ is the maximal value of the gap in $^3\text{He-A}$ which plays the part of the Planck energy, the quasiparticles do obey the relativistic equation

$$g^{\mu\nu}(p_\mu - eA_\mu)(p_\nu - eA_\nu) = 0 \quad (20)$$

Here $e = \pm$ is the "electric charge" and simultaneously the chirality of the quasiparticles. Let us consider the simplest situation, when the ${}^3\text{He-A}$ is in its vacuum manifold, which is characterized by two unit mutually orthogonal vectors $\mathbf{e}^{(1)}$ and $\mathbf{e}^{(2)}$, and neglect the spin degeneracy of the Fermi point. When we consider the low-energy collective modes, these vectors are slowly changing in space-time. In this situation the effective metric and effective electromagnetic field are given by:

$$\mathbf{A} = p_F \hat{\mathbf{l}}, \quad A_0 = p_F \mathbf{v}_s \cdot \hat{\mathbf{l}}, \quad (21)$$

$$g^{ik} = v_F^2 (\delta^{ik} - \hat{l}^i \hat{l}^k) + c^2 \hat{l}^i \hat{l}^k - v_s^i v_s^k, \quad (22)$$

$$g^{00} = -1, \quad g^{0i} = v_s^i,$$

where \mathbf{v}_s is the superfluid velocity given by $v_{si} = (\hbar/2m)\mathbf{e}^{(1)}\nabla_i\mathbf{e}^{(2)}$.

From above equations it follows that the fields, which act on the "relativistic" quasiparticles as electromagnetic and gravitational fields, have very strange behavior. For example, the same texture of the $\hat{\mathbf{l}}$ -vector is felt by quasiparticles as the effective magnetic field $\mathbf{B} = p_F \nabla \times \hat{\mathbf{l}}$ according to Eq.(21) and simultaneously it enters the metric according to Eq.(22). Such field certainly cannot be described by the Maxwell and Einstein equations together. Actually the gravitational and electromagnetic variables coincide in ${}^3\text{He-A}$ only when we consider the vacuum manifold: Outside of this manifold they split. ${}^3\text{He-A}$, as any other fermionic system with Fermi point, has enough number of collective modes to provide the analogs for the independent gravitational and electromagnetic fields. But some of these modes are massive in ${}^3\text{He-A}$. For example the gravitational waves correspond to the modes, which are different from the oscillations of the $\hat{\mathbf{l}}$ -vector. As distinct from the photons (orbital waves – propagating oscillations of the $\hat{\mathbf{l}}$ -vector) the gravitons are massive [20].

All these troubles occur because in ${}^3\text{He-A}$ the main contribution to the effective action for bosonic fields come from the vacuum fermions at the "Planck" energy scale, $E \sim \Delta$. These fermions are far from the Fermi points and their spectrum is nonlinear. That is why in general the effective action is not symmetric.

E. Zero charge effect and Maxwell equations.

There are, however, exclusions, for example, the action for the $\hat{\mathbf{l}}$ -field contains the term with the logarithmically divergent factor $\ln(\Delta/\omega)$ [20]. It comes from the zero charge effect, experienced by the vacuum of the massless fermions for whom the $\hat{\mathbf{l}}$ -field acts as electromagnetic field. Due to its logarithmic divergence this term is dominating at low frequency ω : the lower the frequency the larger is the contribution of the vacuum fermions from

the vicinity of the Fermi point and thus the more symmetric is the Lagrangian for the $\hat{\mathbf{l}}$ -field. As a result, in the very low-energy limit, when the non-logarithmic contributions can be neglected, the effective Lagrangian for the A_μ becomes gauge invariant and even obeys the general covariance:

$$L = \frac{\sqrt{-g}}{24\pi^2} \ln\left(\frac{\Delta^2}{\omega^2}\right) g^{\mu\nu} g^{\alpha\beta} F_{\mu\alpha} F_{\nu\beta}, \quad (23)$$

where $F_{\mu\nu}$ is the strength of the effective electromagnetic field A_μ from Eq.(21) and $g^{\mu\nu}$ is the effective gravitational field from Eq.(22). In this regime the A_μ field does obey the Maxwell equations in a curved space.

F. Why ${}^3\text{He-A}$ is not perfect.

On the other hand the "Einstein" action for $g_{\mu\nu}$ is highly contaminated by many noncovariant terms, which come from the integration over the "nonrelativistic" high energy degrees of freedom at "Planck" scale. In this sense the ${}^3\text{He-A}$, with its given physical parameters, is not a perfect model for quantum vacuum. To remove the polluting noncovariant terms, the integration must be spontaneously cut-off at energies much below the "Planck" scale, $E \ll \Delta$, for example, due to strong quasiparticle relaxation.

The main reason why ${}^3\text{He-A}$ is not a good substance, is that the Fermi points of the left particles, i.e. at $\mathbf{p} = +p_F \hat{\mathbf{l}}$, and the Fermi points of the right particles, i.e. at $\mathbf{p} = -p_F \hat{\mathbf{l}}$, are far from each other in equilibrium. The "perfect" condensed matter would be such where all the Fermi points are at the origin, at $\mathbf{p} = 0$, as it happens in the standard model. However, inspite of the absence of general covariance even in the low-energy corner, many different properties of the physical vacuum with a Fermi point, whose direct observation are still far from realization, can be simulated in ${}^3\text{He-A}$. One of them is the chiral anomaly.

G. Chiral anomaly.

The chiral anomaly is the phenomenon which allows the nucleation of the fermionic charge from the vacuum [36,37]. Such nucleation results from the spectral flow of the fermionic charge through the Fermi point to high energy. Since the flux in the momentum space is conserved, it can be equally calculated in the infrared or in the ultraviolet limits. In ${}^3\text{He-A}$ it is much easier to use the infrared regime, where the fermions obey all the "relativistic" symmetries. As a result one obtains the same anomaly equation, which has been derived by Adler and by Bell and Jackiw for the relativistic systems. The rate of production of quasiparticle number $n = n_R + n_L$ from the vacuum in applied electric and magnetic fields is

$$\partial_\mu J^\mu = \frac{1}{8\pi^2}(e_R^2 - e_L^2)F^{\mu\nu}F_{\mu\nu}^* , \quad (24)$$

Here n_R and n_L is the density of the right and left quasiparticles; e_R and e_L are their charges; and $F_{\mu\nu}^*$ is the dual field strength. Note that the above equation is fully "relativistic". This equation has been verified in $^3\text{He-A}$ experiments [38,39], where the "magnetic" $\mathbf{B} = p_F \vec{\nabla} \times \hat{\mathbf{l}}$ and "electric" $\mathbf{E} = p_F \partial_t \hat{\mathbf{l}}$ fields have been simulated by the space and time dependent $\hat{\mathbf{l}}$ -texture. In particle physics the only evidence of axial anomaly is related to the decay of the neutral pion $\pi^0 \rightarrow 2\gamma$, although the anomaly is much used in different cosmological scenaria explaining an excess of matter over antimatter in the Universe (see review [40]).

H. Degeneracy of Fermi point as the origin of the non-Abelian gauge field.

In $^3\text{He-A}$ the Fermi point (say, at the north pole) is doubly degenerate owing to the ordinary spin $\vec{\sigma}$ of the ^3He atom. This means that in equilibrium the two zeroes, each with the topological invariant $N_3 = -1$, are at the same point in momentum space. Let us find out what can be the consequences of the Fermi point degeneracy. It is clear that the collective motion can split the Fermi points: positions of the two points can oscillate separately. Moreover, since the propagator is now the 4×4 matrix there can be the cross terms. If we neglect the degrees of freedom related to the vierbein then the collective variables of the system with the doubly degenerate Fermi point enter the fermionic propagator as

$$\mathcal{G}^{-1} = \tau^\alpha e_a^\mu (p_\mu - eA_\mu - e\sigma_\alpha W_\mu^\alpha) . \quad (25)$$

The new effective field W_μ^α acts on the chiral quasiparticles as $SU(2)$ gauge field. Thus in this effective field theory the ordinary spin of the ^3He atoms plays the part of the weak isospin [41,20]. The "weak" field W_μ^α is also dynamical and in the leading logarithmic order obeys the Maxwell (actually Yang-Mills) equations.

This implies that the higher symmetry groups of our vacuum can in principle arise as a consequence of the Fermi point degeneracy. For example, the 4-fold degeneracy of the Fermi point (which implies that there are, say, 4 left-handed fermionic species, or 2 left-handed + 2 right-handed) can produce the $SU(4)$ gauge group. In particle physics the collective modes related to the shift of the 4-momentum are discussed in terms of the "generalized covariant derivative" [42,43]. In this theory the gauge fields, the Higgs fields, and Yukawa interactions, all are realized as shifts of positions of the degenerate Fermi point, with degeneracy corresponding to different quarks and leptons.

In the Eq.(25) we did not take into account that dynamically the vierbein can also oscillate differently for

each of the two elementary Fermi points. As a result the number of the collective modes could increase even more. This is an interesting problem which must be investigated in detail. If the degenerate Fermi point mechanism has really some connection to the dynamical origin of the non-Abelian gauge fields, we must connect the degeneracy of the Fermi point (number of the fermionic species) with the symmetry group of the gauge fields. Naive approach leads to extremely high symmetry group. That is why there should be some factors which can restrict the number of the gauge and other bosons. For example there can be some special discrete symmetry between the fermions of the degenerate point, which restricts the number of massless bosonic collective modes. Another source of the reduction of the number of the effective field has been found by Chadha and Nielsen [5]. They considered the massless electrodynamics with different metric (vierbein) for the left-handed and right-handed fermions. In this model the Lorentz invariance is violated. They found that the two metrics converge to a single one as the energy is lowered. Thus in the low-energy corner the Lorentz invariance becomes better and better, and at the same time the number of independent bosonic modes decreases.

Since the connections between QFT in the standard model and in $^3\text{He-A}$ has been discussed in the earlier publications [20,41,39], we concentrate here on some problems related to gravitational analogy.

IV. BLACK HOLE IN $^3\text{HE-A}$ FILM.

A. Gravity by motion of superfluids. Sonic black hole.

As we have seen from Eq.(22) the gravitational field can be simulated in $^3\text{He-A}$ by the motion of the liquid with the superfluid velocity \mathbf{v}_s and by the $\hat{\mathbf{l}}$ -texture [44]. In this Section we consider the situation when the $\hat{\mathbf{l}}$ -vector is uniform and thus does not produce the effective gravitational field, so that the gravitational effects come only from the motion of the superfluid vacuu. The propagation of fermions in the moving liquid obeys the same equation as propagation of relativistic particles in the gravitational field. The same happens for propagating sound waves in normal fluids [45,46] and phonons in superfluid ^4He . In the simplest case of the radial motion of superfluid ^4He , the effective metric is expressed in terms of the radial superfluid velocity $v_s(r)$ as

$$ds^2 = - (c^2 - v_s^2(r)) dt^2 + 2v_s(r) dr dt + dr^2 + r^2 d\Omega^2 , \quad (26)$$

where c now is a speed of sound in ^4He (phonon velocity). For $^3\text{He-A}$ fermions the spherically symmetric metric occurs if $\hat{\mathbf{l}}$ -field is radial. Then it follows from Eq.(22)

$$ds^2 = -(c^2 - v_s^2(r)) dt^2 + 2v_s(r) dr dt + \frac{c^2}{v_F^2} dr^2 + r^2 d\Omega^2, \quad (27)$$

Kinetic energy of superflow plays the part of the gravitational potential: $\Phi = -v_s^2(r)/2$. If one chooses the velocity field corresponding to the potential of the point body of mass M

$$v_s^2(r) = -2\Phi = \frac{2GM}{r} \equiv c^2 \frac{r_h}{r}, \quad (28)$$

one obtains the Panlevé-Gullstrand form of Schwarzschild geometry (see e.g. ref. [46]). Here r_h denotes the position of the event horizon, where the velocity reaches the "speed of light" c . If the fluid moves towards the origin, the low-energy quasiparticles are trapped behind the horizon, since their speed c with respect to the fluid is less than the velocity of the fluid.

Such sonic black hole was first suggested by Unruh for ordinary liquid [45]. However since all the known normal liquids are classical, the most interesting quantum effects related to the horizon cannot be simulated in such flow. Also the geometry is such that it cannot be realized: in such radial flow inward the liquid is accumulated at the origin, so that this sonic black hole cannot be stationary. In the other scenario a horizon appears in moving solitons, if the velocity of the soliton exceeds the local "speed of light" [44]. This scenario has the same drawback: in finite system the motion of the soliton cannot be supported for a long time. In a draining bathtub geometry suggested in Ref. [47] the fluid motion can be made constant in time. However the friction of the liquid, which moves through the drain, is the main source of dissipation. The superfluidity of the liquid does not help much in this situation. Horizon does not appear since the "superluminal" motion with respect to the boundaries of the drain tube is not allowed: The superflow becomes unstable and superfluidity collapses (see [48]). Let us suggest a scenario, in which this collapse is avoided. The superfluid motion becomes quasi-stationary and exhibits the event horizon; the life time of the flow state is determined by Hawking radiation.

B. Simulation of 2D black hole

The stationary black hole can be realized in the following geometry, which is the development of the bathtub geometry of Ref. [47] (see Fig. 3(a)). The superfluid $^3\text{He-A}$ film is moving towards the center of the disk, where it escapes to the third dimension due to the orifice (hole). If the thickness of the film is constant, the flow velocity increases towards the center as $v_s(r) = b/r$ and at $r = r_h = b/c$ reaches the speed of light (now r denotes

2D "sonic" black hole in $^3\text{He-A}$ film

* Panlevé-Gullstrand form of 2D black hole:

$$ds^2 = -dt^2 (c^2 - v^2(r)) + 2v(r) dr dt + dr^2 + r^2 d\phi^2$$

* If $^3\text{He-A}$ film is moving to the hole

$$v(r) = b/r$$

* Horizon is at $r_h = b/c$

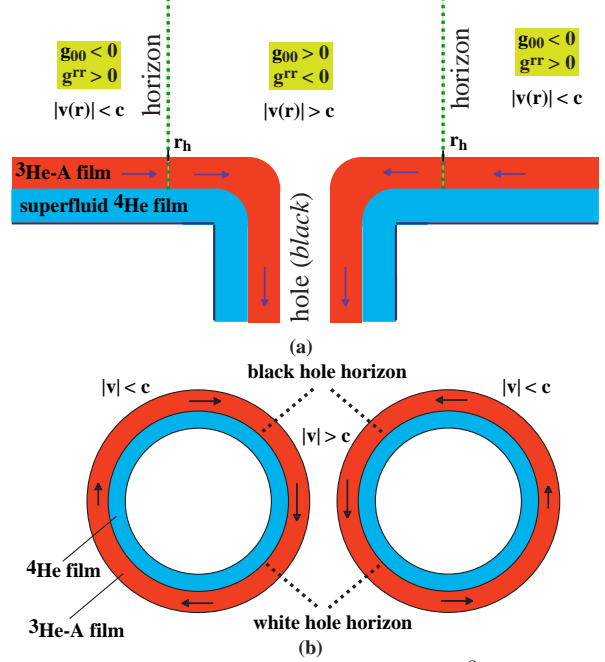


FIG. 3. Simulation of 2D black hole in thin $^3\text{He-A}$ film. (a) Draining bathtub geometry. (b) $^3\text{He-A}$ film circulating on the top of the ^4He film on torus.

the radial coordinate in the cylindrical system). Outside the orifice the motion of the liquid is two dimensional and the effective metric for the low-energy Bogoliubov quasiparticles is

$$ds^2 = -(c^2 - v_s^2) dt^2 + 2v_s dr dt + dr^2 + r^2 d\phi^2 + \frac{c^2}{v_F^2} dz^2. \quad (29)$$

Here we took into account that the \hat{l} vector in the film is fixed along the normal to the film, so that the "speed of light" for quasiparticles propagating along the film $c \sim 3$ cm/sec is much smaller than the Fermi velocity v_F which corresponds to the "speed of light" for quasiparticles propagating along the normal to the film. Note that c is much smaller than the speed of sound in $^3\text{He-A}$, that is why the motion of fluid has no effect on the density of the liquid.

The important element of the construction in Fig. 3 is that the moving superfluid $^3\text{He-A}$ film is placed on the top of the superfluid ^4He film. This is made to avoid the interaction of the $^3\text{He-A}$ film with the solid substrate.

The superfluid ^4He film effectively screens the interaction and thus prevents the collapse of the superfluid flow of $^3\text{He-A}$ with "superluminal" velocity: Since the interactions with walls is removed the local observer moving with the superfluid velocity cannot detect the relative motion with respect to the wall.

The motion of the superfluid $^3\text{He-A}$ with respect to superfluid ^4He film is not dangerous: The superfluid ^4He is not excited even if $^3\text{He-A}$ moves with its superluminal velocity: c for $^3\text{He-A}$ is much smaller than the Landau velocity for radiation of quasiparticles in superfluid ^4He , which is about 50 m/sec. In this consideration we neglected the radiation of surface waves, assuming that the thickness of ^4He film is small enough.

Finally one can close the superflow by introducing the toroidal geometry in Fig. 3(b), so that the superfluid condensate can circulate. In this case in addition to the black hole horizon the white hole horizon appears on the path where the superfluid $^3\text{He-A}$ flows out from the orifice.

Since the extrinsic mechanism of the friction of $^3\text{He-A}$ film – the scattering of quasiparticles on the roughness of substrate – is abandoned, we can consider now intrinsic mechanisms of dissipation. The most interesting one is the Hawking radiation related to existence of a horizon.

C. Vacuum in comoving and rest frames.

Let us consider the simplest case of the 2D motion along the film in the bathtub geometry of Fig. 3(a). This can be easily generalized to the motion in the torus geometry.

There are two important reference frames: (i) The frame of the observer, who is locally comoving with the superfluid vacuum. In this frame the local superfluid velocity is zero, $\mathbf{v}_s = 0$, so that the energy spectrum of the Bogoliubov fermions in the place of the observer is (here we assume a pure 2D motion along the film)

$$E_{\text{com}} = \pm cp . \quad (30)$$

In this geometry, in which the superflow velocity is confined in the plane of the film, the speed c coincides with the Landau critical velocity of the superfluid vacuum, $v_{\text{Landau}} = \min(|E_{\text{com}}(p)|/p)$. The vacuum as determined by the comoving observer is shown on Fig. 4(a): fermions occupy the negative energy levels in the Dirac sea (the states with the minus sign in Eq.(30). It is the counterpart of the Minkowski vacuum, which is however determined only locally: The comoving frame cannot be determined globally. Moreover for the comoving observer, whose velocity changes with time, the whole velocity field $\mathbf{v}_s(\mathbf{r}, t)$ of the superflow is time dependent. This does not allow to determine the energy correctly.

(ii) The energy can be well defined in the laboratory frame (the rest frame). In this frame the system is stationary, though is not static: The effective metric does not depend on time, so that the energy is conserved, but this metric contains the mixed component $g_{0i} = v_{si}$. The energy in the rest frame is obtained from the local energy in the comoving frame by the Doppler shift:

$$E_{\text{rest}} = \pm cp + \mathbf{p} \cdot \mathbf{v}_s(\mathbf{r}) . \quad (31)$$

In case of the radial superflow $\mathbf{v}_s(\mathbf{r}) = \hat{\mathbf{r}}v_s(r)$ one has

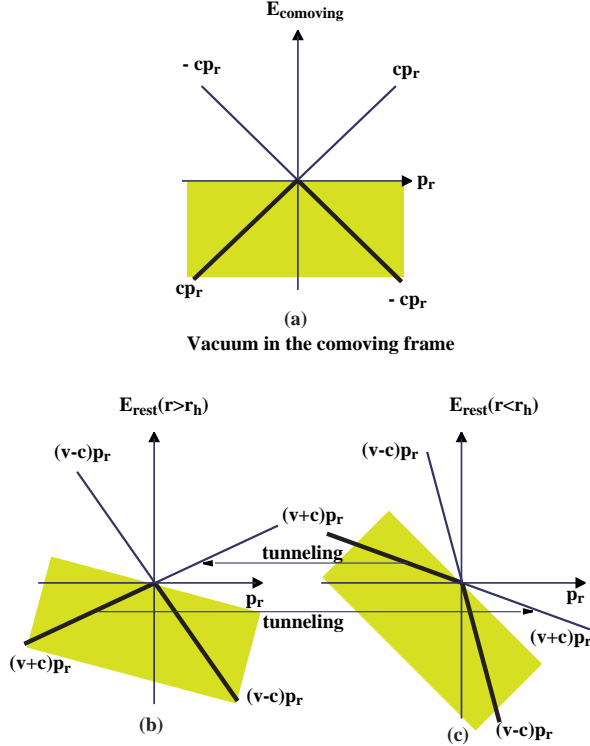
$$E_{\text{rest}} = \pm cp + p_r v_s(r) . \quad (32)$$

Figs. 4(b-c) show how the "Minkowski" vacuum of the comoving frame is seen by the rest observer (note that the velocity is negative, $v_s(r) < 0$). In the absence of horizon, or outside the horizon the local vacuum does not change: the states which are occupied (empty) in the Minkowski vacuum remain occupied (empty) in the rest frame vacuum (see Fig. 4(b)). In the presence of horizon behind which the velocity of superflow exceeds the Landau critical velocity the situation changes: Behind the horizon the vacuum in the rest frame differs from that in the comoving frame. Let us for simplicity consider the states with zero transverse momentum $p_\phi = 0$ on the branch $E_{\text{rest}} = (v_s(r) + c)p_r$ in the rest frame. If the system is in the Minkowski vacuum state (i.e. in the ground state as viewed by comoving observer), quasiparticles on this branch has reversed distribution in the rest frame: the negative energy states are empty, while the positive energy states are occupied (see Fig. 4(c)). For this branch the particle distribution corresponds to the negative temperature $T = -0$ behind horizon.

Since the energy in the rest frame is a good quantum number, the fermions can tunnel across the horizon from the occupied levels to the empty ones with the same energy. Thus if the system is initially in the Minkowski vacuum in the comoving frame, the tunneling disturbs this vacuum state: Pairs of excitations are created: the quasiparticle, say, is created outside the horizon while its partner – the quasihole – is created inside the horizon. This simulates the Hawking radiation from the black hole.

D. Hawking radiation

To estimate the tunneling rate in the semiclassical approximation, let us consider the classical trajectories $p_r(r)$ of particles, say, with positive energy, $E_{\text{rest}} > 0$, for the simplest case when the transverse momentum p_ϕ is zero Fig. 5. The branch $E_{\text{rest}} = (v_s(r) - c)p_r$ describes the incoming particles with $p_r < 0$ which propagate through the horizon to the orifice (or to the singularity at $r = 0$, if the orifice is infinitely small) without any singularity at



The same vacuum viewed in rest frame:
 (b) outside horizon; (c) behind horizon.
 Tunneling occurs from occupied states behind horizon
 to empty states outside horizon

FIG. 4. (a) Fermionic vacuum in the comoving frame. The states with $E_{\text{com}} < 0$ are occupied (thick lines). The same vacuum viewed in the rest frame (b) outside horizon and (c) inside horizon. Behind the horizon the branch $E_{\text{rest}} = (v+c)p_r$ (for $p_{\perp} = 0$) has inverse population as seen in the rest frame: the states with positive energy $E_{\text{rest}} > 0$ are filled, while the states with $E_{\text{rest}} < 0$ are empty. The tunneling across horizon from the occupied states to the empty states with the same energy gives rise to the Hawking radiation from the horizon.

the horizon. The classical trajectories of these particles are

$$p_r(r) = -\frac{E_{\text{rest}}}{c - v_s(r)} < 0. \quad (33)$$

The energies of these particles viewed by the comoving observer are also positive: $E_{\text{com}}(r) = -cp_r(r) = E_{\text{rest}}(1 - (v_s(r)/c))^{-1} > 0$.

Another branch $E_{\text{rest}} = (v_s(r) + c)p_r$ in Fig. 5 contains two disconnected pieces describing the particle propagating from the horizon in two opposite directions:

$$r > r_h : p_r(r) = \frac{E_{\text{rest}}}{c + v_s(r)}, \quad E_{\text{com}}(r) = cp_r(r) > 0 \quad (34)$$

$$r < r_h : p_r(r) = \frac{E_{\text{rest}}}{c + v_s(r)}, \quad E_{\text{com}}(r) = cp_r(r) < 0 \quad (35)$$

Hawking radiation

* Panlevé-Gullstrand form of black hole:

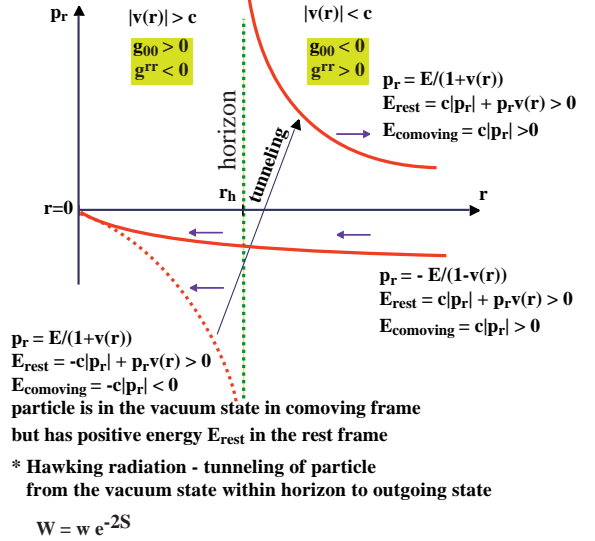
$$ds^2 = -dt^2(c^2 - v^2(r)) + 2v(r) dr dt + dr^2 + r^2 d\Omega^2$$

kinetic energy of flow = gravitational potential: $v^2(r)/2 = GM/r$

* Particle energy in the rest frame $E_{\text{rest}} = \pm c|p| + p_r v(r)$

Particle energy in comoving frame $E_{\text{comoving}} = \pm c|p|$

* Trajectories of particle with positive energy in the rest frame



* Hawking radiation - tunneling of particle
 from the vacuum state within horizon to outgoing state

$$W = w e^{-2S}$$

$$S = \text{Im} \int dr p_r = \pi E / |v'(r_h)| = E / 2T_{\text{Hawking}}$$

FIG. 5. Tunneling from Minkowski vacuum within the horizon to the outgoing mode.

The Eq.(34) describes the outgoing particles – the particles propagating from the horizon to the exterior. The energy of these particles is positive in both frames, comoving and rest. The Eq.(35) describes the propagation of particles from the horizon to the orifice (or to the singularity). Though for the rest frame observer the energy of these particles is positive, these particles, which live within the horizon, belong to the Minkowski vacuum in the comoving frame.

The classical trajectory in Eqs.(34,35) is thus disrupted at the horizon. There is however a quantum mechanical transition between the two pieces of the branch: the quantum tunneling. The tunneling amplitude can be found in semiclassical approximation by shifting the contour of integration to the complex plane:

$$w \sim \exp(-2S), \quad (36)$$

$$S = \text{Im} \int dr p_r(r) = \frac{\pi E_{\text{rest}}}{|v'_s(r)|_{r=r_h}}. \quad (37)$$

This means that the wave function of any particle in the Minkowskii vacuum inside the horizon contains an exponentially small part describing the propagation from the horizon to infinity. This corresponds to the radiation from the Minkowski vacuum in the presence of the event

horizon. The exponential dependence of the probability on the quasiparticle energy E_{rest} suggests that this radiation looks as thermal. The corresponding temperature, the Hawking temperature, is

$$T_{\text{Hawking}} = \frac{\hbar |v'_s(r)|_{r=r_h}}{2\pi} . \quad (38)$$

The radiation leads to the quantum friction: the linear momentum of the flow decreases with time. This occurs continuously until the superfluid Minkowski vacuum between the horizons is completely exhausted and the superfluid state is violated. This leads to the phase slip event, after which the number N_3 of circulation quanta of superfluid velocity trapped by the torus is reduced. This process will repeatedly continue until the two horizons merge.

E. Discussion.

The above construction in Fig. 3(b) allows us (at least in principle) to obtain the event horizon in the quasi-stationary regime, when the main source of nonstationarity is the dissipation coming from the Hawking radiation. As for the practical realization, there are, of course, many technical problems to be solved. On the other hand, if the black hole analog can in principle exist in condensed matter as the quasi-stationary object, its prototype – the real black hole – can also exist, at least in principle (though it is not so easy to find the scenario of how this object can be obtained from the gravitational collapse of matter [49]).

It appears that in some range of the energies of Hawking-radiated particles, close to the "Planck" scale, where the fermionic spectrum becomes "nonrelativistic", the Hawking radiation does not exist any more. The particles which are radiated in the fully relativistic case, will be now Andreev scattered back to the black hole. Thus both partners (particle and hole) of the Hawking radiation will remain within the horizon, so that the particle creation in high gravity field will disturb the quantum vacuum inside the horizon without any radiation outside. In principle the pair creation inside the horizon can be more important for the dissipation in the superfluid ^3He film under discussion than the Hawking radiation.

V. ROTATING VACUUM.

A. Unruh effect.

The body moving in the vacuum with linear acceleration a is believed to radiate the thermal spectrum with the Unruh temperature $T_U = \hbar a / 2\pi c$ [50]. The comoving observer sees the vacuum as a thermal bath with $T = T_U$,

so that the matter of the body gets heated to T_U (see references in [51]). Linear motion at constant proper acceleration (hyperbolic motion) leads to velocity arbitrarily close to the speed of light. On the other hand uniform circular motion features constant centripetal acceleration while being free of the above mentioned pathology (see the latest references in [52–55]). The latter motion is stationary in the rotating frame, which is thus a convenient frame for study of the radiation and thermalization effects for uniformly rotating body.

B. Zel'dovich-Starobinsky effect.

Zel'dovich [56] was the first who predicted that the rotating body (say, dielectric cylinder) amplifies those electromagnetic modes which satisfy the condition

$$\omega - L\Omega < 0 . \quad (39)$$

Here ω is the frequency of the mode, L is its azimuthal quantum number, and Ω is the angular velocity of the rotating cylinder. This amplification of the incoming radiation is referred to as superradiance [57]. The other aspect of this phenomenon is that due to quantum effects, the cylinder rotating in quantum vacuum spontaneously emits the electromagnetic modes satisfying Eq.(39) [56]. The same occurs for any rotating body, including the rotating black hole [58], if the above condition is satisfied.

Distinct from the linearly accelerated body, the radiation by a rotating body does not look thermal. Also, the rotating observer does not see the Minkowski vacuum as a thermal bath. This means that the matter of the body, though excited by interaction with the quantum fluctuations of the Minkowski vacuum, does not necessarily acquire an intrinsic temperature depending only on the angular velocity of rotation. Moreover the vacuum of the rotating frame is not well defined because of the ergoregion, which exists at the distance $r_e = c/\Omega$ from the axis of rotation.

The problems related to the response of the quantum system in its ground state to rotation [52], such as radiation by the object rotating in vacuum [56,59,58,57] and the vacuum instability caused by the existence of ergoregion [60], etc., can be simulated in superfluids, where the superfluid ground state plays the part of the quantum vacuum. The quantum friction due to spontaneous emission of phonons in superfluid ^4He and Bogoliubov fermions in superfluid ^3He -B has been discussed in [61]. Here we extend an analysis to the radiation of quasiparticles in ^3He -A.

C. Cylindrical geometry.

Let us consider a cylinder of radius R rotating with angular velocity Ω in the (infinite) superfluid liquid. In this

situation there are again two important reference frames. One of them is the laboratory frame. The energy of quasiparticles is not well determined in the laboratory frame, because, if the rotating body is not the perfect axysymmetric cylinder, it produces the time dependent perturbations of the liquid. However at distances far enough from the surface of the cylinder the influence of the rotating cylinder on the liquid can be neglected. In this approximation the superfluid vacuum is in rest with respect to the laboratory frame. This means that the superfluid velocity $\mathbf{v}_s = 0$ in the laboratory frame. The quasiparticle energy in this frame is that as in the comoving frame of previous Section. It is $E_{\text{com}} = cp$ if we consider superfluid ${}^4\text{He}$, or the Eq.(30), if we consider a pure 2D motion of ${}^3\text{He-A}$ with $\hat{\mathbf{l}} = \hat{\mathbf{z}}$. Such energy spectrum corresponds to the effective Minkowski metric of flat space

$$ds^2 = -c^2 dt^2 + r^2 d\phi^2 + dr^2 + a^2 dz^2 . \quad (40)$$

Here $a = 1$ for isotropic ${}^4\text{He}$ and $a = c/v_F$ for anisotropic ${}^3\text{He-A}$.

D. Conical texture with negative angle deficit.

In the 3D case of ${}^3\text{He-A}$ there can be another effective metric far from the body. It can be caused by the normal boundary condition on the $\hat{\mathbf{l}}$ -vector, which prefers the radial orientation of $\hat{\mathbf{l}}$ -vector. In the case of the radial distribution, $\hat{\mathbf{l}} = \hat{\mathbf{r}}$, the effective metric for the quasiparticles moving outside the cylinder follows from Eq.(22):

$$ds^2 = -c^2 dt^2 + dz^2 + r^2 d\phi^2 + \frac{c^2}{v_F^2} dr^2 . \quad (41)$$

Such an effective space is conical: The space outside the cylinder is flat, but the proper length of the circumference of radius r around the cylinder is not equal to $2\pi r$. In the relativistic theories such conical metric can arise outside the local cosmic strings, where there is an angle deficit. In our case the length of the circumference is $2\pi r v_F/c$, which is much larger than $2\pi r$: This effective space exhibits a "negative angle deficit" (for details see Ref. [62]).

E. Rotating frame.

Since the system far outside the rotating cylinder is not disturbed by the rotation of the body, the system will remain to be in or close to the Minkowski vacuum (or vacuum in the conical space in the case of radial $\hat{\mathbf{l}}$ -vector) as viewed in the laboratory frame. However this does not hold in the region adjacent to the cylinder, where the superfluid velocity field is disturbed and time-dependent. Also the energy in the laboratory frame is not well determined because of the time-dependent perturbations.

The energy is well determined in the frame corotating with the cylinder. In the corotating frame the cylinder is at rest, and thus the perturbations caused by rotation are stationary. The metric in the corotating frame is simplest far outside the rotating body, where the superfluid velocity in the corotating frame is $\mathbf{v}_s = -\vec{\Omega} \times \mathbf{r}$. Substituting this \mathbf{v}_s into Eq.(22) one obtains the interval $ds^2 = g_{\mu\nu} dx^\mu dx^\nu$, which determines the propagation of quasiparticles in the corotating frame:

$$ds^2 = -(c^2 - \Omega^2 r^2) dt^2 - 2\Omega r^2 d\phi dt + r^2 d\phi^2 + dr^2 + a^2 dz^2 . \quad (42)$$

Here again $a = 1$ for phonons in isotropic ${}^4\text{He}$ and $a = c/v_F$ for fermionic quasiparticles in anisotropic ${}^3\text{He-A}$ with $\hat{\mathbf{l}} = \hat{\mathbf{z}}$. These metrics correspond to the interval in the rotating frame discussed in relativistic theories.

It is convenient to write the quasiparticle spectrum in this frame in two different approximations. In classical description one has $E_{\text{corotating}} = E_{\text{com}}(\mathbf{p}) + \mathbf{p} \cdot \mathbf{v}_s$. In the other description, an azimuthal motion of quasiparticles is quantized in terms of the angular momentum $L = rp_\phi$, while the radial is still treated in the quasiclassical approximation. In this case the energy spectrum of phonons in the corotating frame is

$$E_{\text{corotating}} = cp + \mathbf{p} \cdot \mathbf{v}_s = c\sqrt{\frac{L^2}{r^2} + p_z^2 + p_r^2} - \Omega L , \quad (43)$$

and the energy spectrum of the Bogoliubov fermions

$$E_{\text{corotating}}(\mathbf{p}) = \pm\sqrt{\frac{c^2}{r^2} L^2 + c^2 p_r^2 + v_F^2 (p_z \mp p_F)^2} - \Omega L . \quad (44)$$

F. Ergoregion in superfluids.

The radius $r_e = c/\Omega$, where $g_{00} = 0$ in the Eq.(42), marks the position of the ergoplane. In the ergoregion, i.e. at $r > r_e = c/\Omega$, the energy of quasiparticle in Eq.(44) can be negative for any $L \geq 1$. This means that in the ergoregion the Minkowski vacuum is not the vacuum for the corotating observer. Situation is similar to the case discussed in previous Section. However the relevant superfluid velocity is azimuthal now instead of radial. As a result there is an ergoplane instead of a horizon.

From the point of view of the corotating observer, the Minkowski vacuum is unstable towards the filling of the negative energy states in the ergoregion, which means the radiation of the quasiparticles from the rotating cylinder. However we need a real process, which leads to such radiation. This radiation can be caused only by the interaction between the superfluid Minkowski vacuum and the rotating object.

Let us consider the slow rotations $\Omega R \ll c$. In this case the linear velocity of the cylinder at the surface of the cylinder, ΩR , is much smaller than the Landau critical velocity for nucleation of quasiparticles, $v_{Landau} = c$. Thus quasiparticles cannot be nucleated near the surface of cylinder. The ergoregion, where $|v_s| = \Omega r > c$ and quasiparticles can be nucleated, is far from the cylinder, $r_e \gg R$. The interaction with the cylinder, which produces the matrix element for the radiation, is very small. In this situation the most effective mechanism of the quasiparticle radiation is the tunneling of quasiparticles from the liquid adjacent to the surface of the rotating body, which plays the part of the rotating detector, to the ergoregion.

G. Rotating detector.

The simplest rotating detector is the fermionic system, which is rigidly connected to the rotating body. In superfluids the rotating body can be effectively substituted by the rigidly rotating cluster of quantized vortices (see Fig. 6(a)). Such clusters, that experience the solid-body rotation, are experimentally investigated in both phases of superfluid ^3He (see e.g. [63]). The vortex cluster rotating in the infinite superfluid liquid represents the vacuum in the corotating frame. However this vacuum state is not extended to the exterior of the cluster, where one has the analogue of Minkowski vacuum. That is why such state is not equilibrium, but it is quasistationary metastable state which can live for a macroscopically long time. At $T = 0$ the dominating mechanism of the relaxation of angular velocity Ω of the cluster is the process of the radiation of quasiparticles.

Fig. 6(b) shows the distribution of superfluid velocity v_s in the laboratory frame. Within the vortex cluster, i.e. at $r < R$, the superfluid velocity, being averaged over the vortices, follows the velocity of the solid body rotation of the cluster: i.e. $\langle \mathbf{v}_s \rangle = \vec{\Omega} \times \mathbf{r}$ in the laboratory frame and thus $\langle \mathbf{v}_s \rangle = 0$ in the frame corotating with the cluster. Outside the cluster the superfluid velocity decays as $N\kappa/2\pi r$, where N is number of vortices in the cluster and κ is superfluid circulation around individual vortex.

Within the cluster one has $\langle \mathbf{v}_s \rangle = 0$ in the corotating frame, so one can expect that the spectrum of quasiparticles, which live within the cluster, is the same as the energy spectrum in the frame comoving with the superfluid velocity, $E_{\text{corotating}} = E_{\text{com}}$. In other words this spectrum has no $-\Omega L$ shift of the energy levels, as distinct from quasiparticle spectrum far from the body, Eqs.(43,44), which is measured in the same corotating frame. This is not exactly true, since the equation $\langle \mathbf{v}_s \rangle = 0$ does not imply that $\mathbf{v}_s = 0$ locally: it essentially depends on the position in the vortex lattice.

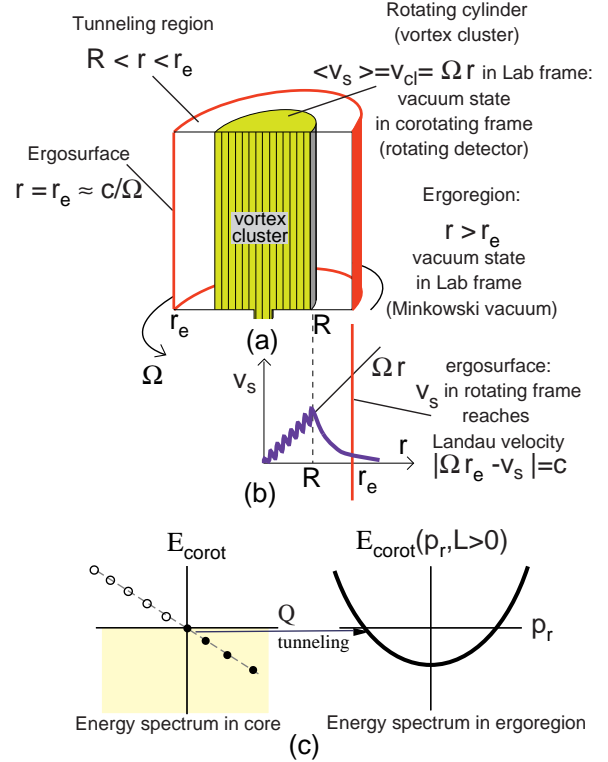


FIG. 6. (a) Rotating body – rigidly rotating cluster of vortices. Within the cluster, at $r < R$, the average superfluid velocity equals the velocity v_{cl} of the solid body rotation of the cluster. Superfluid state within the cluster plays the part of rotating detector: this is the vacuum state in the corotating frame. Far outside of the cluster, where velocity of the superfluid is zero in the Lab frame, the system is in Minkowski vacuum. (b) Distribution of the superfluid velocity in the laboratory frame. At $r = r_e \approx c/\Omega$ the superfluid velocity in the corotating frame reaches the "speed of light" – the Landau critical velocity $v_{Landau} = c$. At $r > r_e$ there is an ergoregion in the corotating frame, where the quasiparticle negative energy states are empty. (c) Tunneling of quasiparticles from the vacuum state of the rotating detector to the "Minkowski" vacuum in the ergoregion. This produces radiation from the rotating body (from vortex cluster) and excitation of the rotating detector (the fermion zero modes in the cores of vortices)

The main feature is nevertheless preserved, when one considers the spectrum of quasiparticles that live in the vortex core. Their energy spectrum in the corotating state does not depend on rotation velocity Ω : $E_{\text{corotating}} = -\omega_0(p_z)Q$, where Q is the generalized angular momentum; $\omega_0(p_z)$ is the so called minigap, which depends on the core structure. This branch crosses zero energy level as a function of Q , if one considers this quantum number as continuous, and thus represents the fermion zero mode (see left part of Fig. 6(c)). The energy spectrum of such chiral fermions, that live in the vortex core, has been first calculated by Caroli, de Gennes

and Matricon for the Abrikosov vortex in s -wave superconductors [64]; on the relation between the number of fermion zero modes and the winding number of the vortex see [65]. For us it is important that for vortices in ^3He the quantum number Q is integer and thus one has the states in the detector with zero energy in the corotating frame.

H. Radiation to the ergoregion.

The radiation of Bogoliubov quasiparticles can be considered as the process in which the particle from the zero energy state in the detector, $E_{\text{corotating}} = 0$, tunnels to the scattering state at the ergoplane, where also its energy is $E_{\text{corotating}} = 0$ (Fig. 6(c)). In the quasiclassical approximation the tunneling probability is e^{-2S} , where at $p_z = \pm p_F$ and $\Omega R \ll c$:

$$S = \text{Im} \int dr p_r(r; E = 0) = L \int_R^{r_e} dr \sqrt{\frac{1}{r^2} - \frac{1}{r_e^2}} \approx L \ln \frac{r_e}{R}. \quad (45)$$

Thus all the particles with $L > 0$ are radiated, but the radiation probability is smaller for higher L :

$$w \propto e^{-2S} = \left(\frac{R}{r_e}\right)^{2L} = \left(\frac{\Omega R}{c}\right)^{2L} = \left(\frac{\omega R}{cL}\right)^{2L}, \quad \Omega R \ll c. \quad (46)$$

Here $\omega = \Omega L$ is energy (frequency) of the radiated quasiparticles in the laboratory frame.

If c is substituted by the speed of light, Eq.(46) is proportional to the superradiant amplification of the electromagnetic waves by rotating dielectric cylinder derived by Zel'dovich [57,59].

Since each radiated fermion carries the angular momentum L , the vortex cluster rotating in superfluid vacuum at $T = 0$ is losing its angular momentum and thus experiences the quantum rotational friction. The radiation also leads to excitation of the detector matter. In principle the radiation can occur without excitation of the detector vacuum, via direct interaction of the particles in the Minkowski vacuum with the rotating body (cluster), but the contribution of this process the quantum friction is smaller [61].

I. Discussion.

The rotational friction experienced by the body rotating in superfluid vacuum at $T = 0$, is caused by the spontaneous quantum emission of the quasiparticles from the rotating object to the "Minkowski" vacuum in the ergoregion. The emission is not thermal and depends on

the details of the interaction of the radiation with the rotating body. In the quasiclassical approximation it is mainly determined by the tunneling exponent, which can be approximately characterized by the effective temperature $T_{\text{eff}} \sim \hbar\Omega(2/\ln(c/\Omega R))$. The vacuum friction of the rotating body can be observed only if the effective temperature exceeds the temperature of the bulk superfluid, $T_{\text{eff}} > T$. For the body rotating with $\Omega = 10^3 \text{rad/s}$, T must be below 10^{-8}K . However, high rotation velocity can be obtained for clusters. The cluster containing two vortices rotate around their center of mass with $\Omega = \kappa/4\pi R^2$, where R is the radius of the circular orbit. If the radius R is of order of superfluid coherence length, the effective temperature can reach 10^{-4}K .

The process discussed in this Section occurs only if there is an ergoplane in the rotating frame. If the superfluid is contained in a finite external cylinder of radius $R_{\text{ext}} > R$, this process occurs only at high enough rotation velocity, $r_e(\Omega) = c/\Omega < R_{\text{ext}}$, when the ergoplane is within the superfluid. On the instability of the ergoregion in quantum vacuum towards emission see also in Ref. [60].

If $r_e(\Omega) > R_{\text{ext}}$ and ergoregion is not present, then the interaction between the coaxial cylinders via the vacuum fluctuations becomes the main mechanism for dissipation. This causes the dynamic Casimir forces between the walls moving laterally (see Review [66]). As in [66] the nonideality of the cylinders, i.e. violation of the rotational symmetry by the body, is the necessary condition for quantum friction.

VI. DISCUSSION

In the above examples of the nontrivial space, the effective gravitational field acts as a fixed external field. The dynamics of this field has not been discussed here. In most cases the effective gravity field do not obey the Einstein equations. This is the main drawback of superfluid $^3\text{He-A}$: Since the Fermi points in $^3\text{He-A}$ are too far apart from each other, the dynamical equations for the gravitational field are clumsy. Nevertheless the above textures allow us to simulate many phenomena related to quantum vacuum in the presence of the strong gravity field. This is because many properties of the quantum vacuum in curved space, which are determined by the geometry, do not depend on the dynamical origin of the geometry. For example, it is well known that the Hawking radiation is a purely kinematic effect and occurs in any geometry, if it exhibits an event horizon [46]. That is why the $^3\text{He-A}$ quantum vacuum is a right object for simulation of many aspects of physics of vacuum in a curved space. For example what is the effect of the breakdown of the Lorentz invariance at higher energy on Hawking radiation. The entropy of the black hole can be also investigated using the above model, since the microstates within the horizon

are well determined and (at least in principle) are completely known in the whole energy range including the "transPlanckian" region. All these are different aspects of the problem of stability of the vacuum in strong gravitational and other fields. The superfluids provide many examples of the instability of the superfluid vacuum, and thus allow us to investigate different mechanisms of relaxation of the physical vacuum – the ether.

-
- [1] Hu, B.L. (1988) 3rd Asia-Pacific Conf. Proceedings, Physics **1**, 301 - 314.
- [2] Wilczek, F. (1998) *Int. J. Mod. Phys. A* **13**, 863 - 886; (1998) *Phys. Today* 11 - 13.
- [3] Jegerlehner, F. (1999) Proceedings of 31st International Ahrenschoop Symposium on the Theory of Elementary Particles, Buckow, Germany, 2 - 6 Sep 1997, Theory of elementary particles, 386 - 392.
- [4] Jackiw, R. (1998) *Proc. Natl. Acad. Sci. USA* **95**, 12776 - 12778.
- [5] Chadha, S. & Nielsen, H.B. (1983) *Nucl. Phys. B* **217**, 125 - 144.
- [6] Hu, B.L. (1996) Expanded version of an invited talk at 2nd International Sakharov Conference on Physics, Moscow, 20 - 23 May 1996, e-Print Archive: gr-qc/9607070
- [7] Volovik, G.E. & Mineev, V.P. (1982) *Sov. Phys. JETP* **56**, 579 - 586.
- [8] Grinevich, P.G. & Volovik, G.E. (1988) *J. Low Temp. Phys.* **72**, 371 - 380.
- [9] G.E. Volovik (1991) *JETP Lett.* **53**, 222 - 225.
- [10] K.B. Blagoev and K.S. Bedell "Luttinger theorem in one dimensional metals", cond-mat/9611240.
- [11] X. G. Wen (1990) *Phys. Rev. B* **42**, 6623-6630.
- [12] H.J. Schulz, G. Cuniberti & P. Pieri, "Fermi liquids and Luttinger liquids", cond-mat/9807366.
- [13] V.M. Yakovenko *Phys. Rev. B* **47**, 8851-8857 (1993).
- [14] Nambu, Y. & Jona-Lasinio, G. (1960) *Phys. Rev.* **122**, 345 - 358; **124**, 246 - 254.
- [15] Alford, M., Rajagopal, K. & Wilczek, F. (1998) *Phys. Lett. B* **422** 247-256; Wilczek, F. (1998) *Nucl. Phys. A* **642**, 1 - 13.
- [16] Ruutu, V.M.H., Eltsov, V.B., Gill, A.J., Kibble, T.W.B., Krusius, M., Makhlin, Yu.G., Placais, B., Volovik, G.E. & Wen Xu, (1996) *Nature* **382**, 334 - 336.
- [17] Kibble, T.W.B. *J. Phys. A* (1976) **9**, 1387 - 1398.
- [18] K. Ishikawa, *Nucl. Phys B* **280**, 523-548 (1987).
- [19] G.E. Volovik, V.M. Yakovenko, *J. Phys.: Cond. Matter* **1**, 5263-5274 (1989).
- [20] Volovik, G.E. (1992) *Exotic properties of superfluid ³He*, World Scientific, Singapore.
- [21] G. E. Volovik, *JETP Lett.* **66** , 522-527 (1997).
- [22] Abrikosov, A.A. (1998) *Phys. Rev. B* **58**, 2788 - 2794.
- [23] Ding, H. et al (1996) *Phys. Rev.*, **B 54**, 9678.
- [24] G.E. Volovik (1997) *JETP Lett.* **65** , 491-496.
- [25] Revaz, B., Genoud, J.-Y., Junod, A., Meumaier, K., Erb, A. & Walker, E. (1998) *Phys. Rev. Lett.*, **80**, 3364 - 3367.
- [26] Volovik, G.E. & Gor'kov, L.P. (1985) *Sov. Phys. JETP* **61**, 843 - 854 (1985).
- [27] Pokrovsky, S.V. & Pokrovsky, V.L. (1995) *Phys. Rev. Lett.*, **75**, 1150 - 1153.
- [28] Sun, Y. & Maki, K. (1995) *Europhys. Lett.* **32**, 355.
- [29] Nersesyan, A.A., Tsvelik, A.M. & Wenger, F. (1994) *Phys. Rev. Lett.*, **72**, 2628 - 2631.
- [30] Lee, P. (1993) *Phys. Rev. Lett.* **71**, 1887 - 1890.
- [31] Sakharov, A.D. *Sov. Phys. Doklady* **12**, 1040 (1968).
- [32] Zeldovich, Ya.B. (1967) *Pis'ma ZhETF* **6**, 922 - 924 [*JETP Lett.* **6**, 345 - 347].
- [33] Mannheim, P.D. (1998) *Phys. Rev. D* **58**, 103511.
- [34] Edery, A. & Paranjape, M.B. (1998) *Phys. Rev. D* **58**, 024011.
- [35] Mannheim, P.D., "Cosmic acceleration and a natural solution to the cosmological constant problem", gr-qc/9903005.
- [36] Adler, S. (1969) *Phys. Rev.* **177**, 2426 - 2438.
- [37] Bell, J.S. & Jackiw, R. (1969) *Nuovo Cim.* **A60**, 47 - 61.
- [38] Bevan, T.D.C., Manninen, A.J., Cook, J.B., Hook, J.R., Hall, H.E., Vachaspati, T. & Volovik, G.E. (1997) *Nature* **386**, 689 - 692.
- [39] Volovik, G.E. (1998) *Physica B* **255**, 86 - 107.
- [40] Trodden, M. (1999) *Rev. Mod. Phys.* to be published, e-Print Archive: hep-ph/9803479.
- [41] Volovik, G.E. & Vachaspati, T. (1996) *Int. J. Mod. Phys. B* **10**, 471 - 521.
- [42] Martin, C.P., Gracia-Bondia, J.M. & Vriilly, J.S. (1998) *Phys. Rep.* **294**, 363 - 406.
- [43] Sogami, I.S. (1995) *Prog. Theor. Phys.* **94**, 117; (1996) *Prog. Theor. Phys.* **95**, 637.
- [44] Jacobson, T.A. & Volovik, G.E. (1998) *Phys. Rev. D* **58**, 064021; (1998) *Pisma ZhETF* **68**, 833 - 838.
- [45] W.G. Unruh, *Phys. Rev. Lett.* **46**, 1351 (1981).
- [46] M. Visser, "Acoustic Black Holes", gr-qc/9901047.
- [47] M. Visser, *Class. Quant. Grav.* **15**, 1767 (1998).
- [48] N.B. Kopnin and G.E. Volovik, *JETP Lett.* **67**, 140 (1998).
- [49] C. Callan, S. Giddings, J. Harvey, and A. Strominger, *Phys. Rev. D* **45** , 1005 (1992).
- [50] W. G. Unruh, *Phys. Rev. D* **14**, 870 (1976).
- [51] J. Audretsch and R. Müller, *Phys. Rev. A* **50**, 1755 (1994).
- [52] P.C.W. Davies, T. Dray, C.A. Manogue, *Phys.Rev. D* **53**, 4382 (1996).
- [53] J.M. Leinaas, "Accelerated Electrons and the Unruh Effect" hep-th/9804179.
- [54] W. G. Unruh, "Acceleration Radiation for Orbiting Electrons" hep-th/9804158.
- [55] D. Barber, "IV. Unruh Effect, Spin Polarisation and the Derbenev-Kondratenko Formalism", physics/9901043.
- [56] Ya.B. Zel'dovich, *Pis'ma ZhETF* **14**, 270, (1971) [*JETP Lett.* **14**, 180, (1971)].
- [57] J.D. Bekenstein and M. Schiffer, *Phys.Rev. D* **58**, 064014 (1998).
- [58] A.A. Starobinskii, *ZhETF*, **64**, 48 (1973) [*JETP*, **37**, 28 (1973)].
- [59] Ya.B. Zel'dovich, *ZhETF*, **62**, 2076 (1971) [*JETP* **35**, 1085 (1971)]
- [60] G. Kang, *Phys. Rev. D* **55**, 7563 (1997).

- [61] A. Calogeracos, and G.E. Volovik, cond-mat/9901163, Pis'ma ZhETF **69**, 257 (1999).
- [62] G.E. Volovik, JETP Lett. **67**, 698 - 704 (1998).
- [63] Ü. Parts, V.M.H. Ruutu, J.H. Koivuniemi, et. al., Europhys. Lett. **31**, 449 (1995).
- [64] C. Caroli, P.G. de Gennes, and J. Matricon, Phys. Lett. **9**, 307 (1964).
- [65] G.E. Volovik, (1993) *JETP Lett.* **57**, 244.
- [66] M. Kardar and R. Golestanian, "The 'Friction' of Vacuum, and other Fluctuation-Induced Forces", cond-mat/9711071.